Inter-Injection-Locked Oscillators for Power Combining and Phased Arrays

KARL D. STEPHAN, MEMBER, IEEE

Abstract—**This paper presents a novel approach to synchronizing the phases of several oscillators for coherent power combining either in a conventional power-combining circuit or in free space as each oscillator drives an antenna element in a phased array. A set of nonlinear differential equations is derived to predict the system's behavior. These equations are used in the computer-aided design and construction of a demonstration three-oscillator inter-injection-locked system at VHF. Good qualitative agreement between initial experimental results and theoretical predictions is observed, and applications of the inter-injection-locking concept to systems are discussed.**

I. Introduction

IN THE DESIGN of microwave systems with solid-state components, the need often arises for more microwave power than a single device can supply. If power from two or more devices is combined to achieve the total power goal, steps must be taken to insure that the outputs of the individual devices are all in phase. The topic of this paper is a novel circuit which controls the output phase of each device with a unique method of injection locking. By coupling adjacent single-device oscillators with suitably designed networks, an entire system of many oscillators can be controlled in phase by a much smaller number of injection-locking input signals. We have chosen to term this method of phase control "inter-injection-locking." In addition, limited phase steering of the oscillators can be performed to generate signals suitable for directly driving elements of a phased-array antenna. Our method differs from earlier applications of injection locking to phased arrays [1] in that we take advantage of inter-oscillator coupling, which was formerly viewed as undesirable. Used within its capabilities, the inter-injection-locking concept can eliminate all but one phase shifter from a linear phased-array transmitting system. At higher microwave frequencies, where conventional phase shifters become increasingly lossy, a minimum number of phase shifters is advantageous.

We will begin with a brief review of single-oscillator injection locking. Existing theory will be extended to encompass the inter-injection-locked circuit topology with multiple oscillators, and results of computer simulations will be presented to show the advantages and limitations of this approach. Limited resources prevented experimental confirmation of results beyond the construction of a rudimentary three-oscillator system at VHF. However, this system successfully demonstrated the basic effects of inter-injection-locking and phase steering. Finally, computer simulations will be used to explore some of the applications of this concept in practical systems.

Manuscript received March 3, 1986; revised June 5, 1986.

The author is with the Department of Electrical and Computer Engineering, University of Massachusetts, Amherst, MA 01003

IEEE Log Number 8609961

II. Injection Locking

A. Review

Examples of oscillating mechanical systems that fall into synchronism with an external periodic force have been known for many years. Adler [2] was one of the first to study electronic oscillator locking phenomena. He developed an expression for the frequency range over which an oscillator will remain locked in phase to an injected signal. Mackey [3] extended Adler's analysis to include effects of phase modulation on the injected signal and showed that injection-locked amplifiers had some significant advantages over conventional amplifiers in the microwave region.

The advent of solid-state negative-resistance devices led to a number of studies by Kurokawa [4]–[6] dealing with various aspects of injection locking of oscillators which use one or more active two-terminal devices. His multiple-device oscillator models summed the power from each device at a common node from which the combined output was removed. This configuration has led to the development of single-cavity injection-locked oscillators and amplifiers working well into the EHF frequency region, where three-terminal devices become too inefficient.

Unlike such single-mode cavity power-combining techniques, we assume in the inter-injection-locking approach that each oscillator is a complete unit and may be coupled to adjacent units in a controlled fashion. Planar circuit technology makes this assumption valid under most circumstances. In our analysis of inter-injection-locked oscillators, we will begin with dual versions of expressions originally derived by Kurokawa. We use these to find a set of differential equations for the amplitude and phase of each oscillator, and then integrate the expressions numerically in time. While this approach may lack elegance when compared to the eigenvalue methods used by Kurokawa and others, it is easily adapted to nonsymmetric systems with unmatched components. Time-domain analysis also lends itself readily to studies of transient phenomena, such

0018-9480/86/1000-1017$01.00 ©1986 IEEE

as the effects of phase slewing and modulation of the injection inputs.

B. Analysis of Single Oscillator

The canonical oscillator circuit we will analyze is shown in Fig. 1. We begin with an assumption about the nature of the output terminal voltage $v(t)$. Let

$$v(t) = A(t)\cos[\omega_i t + \phi(t)] \tag{1}$$

where the peak voltage amplitude $A(t)$ and the instantaneous phase $\phi(t)$ are both slowly varying functions of time. This assumption of a cosinusoidal waveform is reasonably valid in oscillators having resonant circuits whose Q is high enough to short out oscillator harmonics. The phase is measured with respect to an injection signal frequency ω_i, and the modifier "slowly" refers to the rate of change with respect to one period of the injection frequency. The assumption of slowly varying amplitude and phase allows us to neglect higher order terms in the subsequent algebra.

The oscillator circuit model contains an active element representing the active device's dynamic admittance, and passive elements representing both reactive and dissipated energy in the oscillator's resonant structure. The active element's admittance $Y_D(A) = -G_D(A) + jB_D(A)$ depends on the peak amplitude A of the voltage v across its terminals. Reactive energy is stored in an equivalent tank circuit consisting of inductance L and capacitance C. Losses are modeled by the load conductance G_L. Many common two- and three-terminal oscillators may be modeled by the equivalent circuit[1] of Fig. 1 for purposes of inter-injection-locking system design. The following discussion is a dual form of Kurokawa's analysis [4].

The injection signal $i(t)$ in Fig. 1 is a current which, by Kirchhoff's current law, is the sum of the currents through the various components

$$C\frac{dv}{dt} + G_L v + \frac{1}{L}\int v\,dt + Y_D v = i(t). \tag{2}$$

When (1) is substituted into (2), integration by parts yields

$$\begin{aligned} C\left\{-A\left[\omega_i + \frac{d\phi}{dt}\right]\sin(\omega_i t + \phi) + \frac{dA}{dt}\cos(\omega_i t + \phi)\right\} \\ + (G_L - G_D)[A\cos(\omega_i t + \phi)] - B_D A\sin(\omega_i t + \phi) \\ + \frac{1}{L}\left\{\left(\frac{A}{\omega_i} - \frac{A}{\omega_i^2}\frac{d\phi}{dt}\right)\sin(\omega_i t + \phi) \right. \\ \left. + \frac{1}{\omega_i^2}\frac{dA}{dt}\cos(\omega_i t + \phi)\right\} = i \end{aligned} \tag{3}$$

in which the time dependence of A and ϕ have been omitted for brevity. We observe in (3) that $i(t)$ can be expressed as the sum of a cosinusoidal in-phase component of magnitude $I_c(t)$ plus a quadrature sinusoidal component of magnitude $I_s(t)$

$$i(t) = I_c(t)\cos(\omega_i t + \phi) + I_s(t)\sin(\omega_i t + \phi). \tag{4}$$

Using the tank circuit's resonant frequency $\omega_0 = 1/\sqrt{LC}$, we define an injection frequency deviation $\Delta\omega = \omega_i - \omega_0$. Equating sine and cosine terms then leads to differential equations for the amplitude and phase of the oscillator voltage

$$\frac{d\phi}{dt} = -\Delta\omega - \frac{B_D}{2C} - \frac{I_s}{2CA} \tag{5}$$

$$\frac{dA}{dt} = \frac{A}{2C}(G_D - G_L) + \frac{I_c}{2C}. \tag{6}$$

In the absence of injection current ($I_c = I_s = 0$), eq. (6) shows that the steady-state amplitude A_0 is reached when $G_D(A) - G_L = 0$, making $dA/dt = 0$. It is also seen that the in-phase component I_c of the injection current has a first-order effect on amplitude, while instantaneous frequency ($= d\phi/dt$) is primarily influenced by the quadrature component I_s.

C. Analysis of Coupled Oscillators

Suppose that several canonical oscillators are now coupled in a ladder network as shown in Fig. 2. Except for the end oscillators, each circuit is coupled to its two nearest neighbors only,[2] through coupling admittances $Y_c = G_c + jB_c$. Each oscillator's amplitude A_i and phase ϕ_i is indicated, and (5) and (6) give the current–voltage relation in time for each oscillator circuit; the nonlinear nature of the

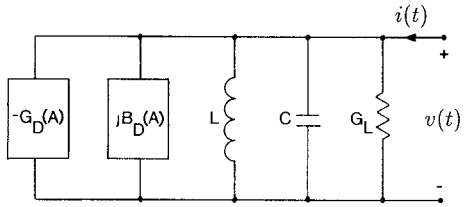

Fig. 1. Canonical oscillator circuit

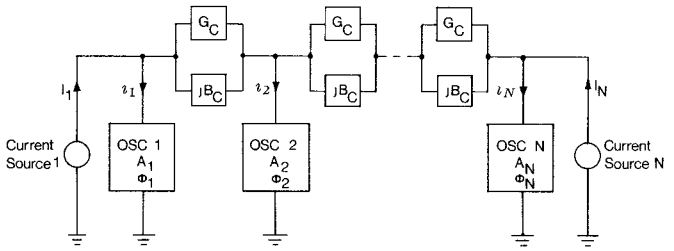

Fig. 2. Canonical oscillator circuits in inter-injection-locked cascade.

[1] While we have chosen to sum the component currents in a parallel circuit, Kurokawa's canonical oscillator circuit is a series loop in which component voltages are summed. Either approach will lead to the same conclusions, although some oscillators may be better modeled with a series circuit.

[2] Other coupling schemes are possible, and general expressions for any coupling network whose Y-matrix exists have been derived. Although such a general formulation is necessary for the analysis of planar phased arrays, etc., the present network has the advantage of mathematical simplicity and applicability to linear phased arrays in which coupling beyond adjacent elements can be neglected.

oscillators precludes their replacement by simple invariant lumped admittances. The phase reference for the cascade has been arbitrarily selected to be the left-hand injection source, which sources a cosinusoidal current of peak amplitude I_1 at a phase $\theta_0 \equiv 0$. The right-hand injection source's amplitude is I_N and its phase is θ_N.

The analysis begins with an assumption of initial conditions for all the amplitudes A_i and phases ϕ_i. (In an actual circuit, the starting amplitudes are near the thermal noise floor and the phases are randomized, but a well-designed circuit will not be dependent upon initial conditions for proper operation.) Given these initial conditions, it is a simple matter to calculate the resulting currents $i_1, i_2, \cdots, i_N$ and find their in-phase and quadrature components *with respect to each oscillator*. Equations (5) and (6) can then be solved for the time evolution of the system. In the following expressions, subscripts have been added to indicate the ith oscillator's amplitude, phase, injection current, and component values:

$$\frac{d\phi_i}{dt} = -\Delta\omega_i - \frac{B_{Di}}{2C} - \frac{1}{2C}\left\{2B_c + \frac{A_{i-1}}{A_i}\left[G_c \sin(\phi_i - \phi_{i-1}) - B_c \cos(\phi_i - \phi_{i-1})\right] + \frac{I_i}{A_i}\sin(\phi_i - \theta_i) + \frac{A_{i+1}}{A_i}\left[G_c \sin(\phi_i - \phi_{i+1}) - B_c \cos(\phi_i - \phi_{i+1})\right]\right\} \quad (7)$$

$$\frac{dA_i}{dt} = \frac{1}{2C}\{A_i(G_{Di} - G_{Li} - 2G_c) + I_i \cos(\phi_i - \theta_i) + A_{i-1}\left[G_c \cos(\phi_i - \phi_{i-1}) + B_c \sin(\phi_i - \phi_{i-1})\right] + A_{i+1}\left[G_c \cos(\phi_i - \phi_{i+1}) + B_c \sin(\phi_i - \phi_{i+1})\right]\}. \quad (8)$$

For the cases we have examined thus far, the numerical integration of the above expressions has generally been straightforward. A typical numerical integration carried to the point of a stable solution takes from 5 to 30 s of CPU time on a VAX 11/750, making an interactive program quite practical. Two reasons for this are 1) the equations exhibit no singularities or other pathological behavior and 2) neglecting the active device reactance B_D leads to simplified expressions. In oscillator circuits whose free-running frequency is substantially independent of device characteristics, setting $B_D = 0$ is a valid approximation and is done throughout the remainder of this paper. Future studies in which the device susceptance becomes significant can include its effects if necessary.

III. Inter-Injection-Locked Oscillators: Experiments

We will now describe the design, analysis, and construction of a prototype inter-injection-locked oscillator system. The goal was to demonstrate that a three-oscillator system could be steered in phase through the use of only one phase shifter. This goal was met, although exact quantitative agreement between theory and the initial experiments was not obtained. Nevertheless, the basic system behavior was predicted well in a qualitative way.

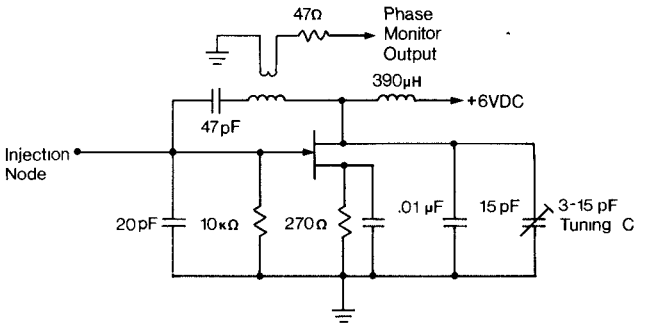

Fig. 3. Experimental VHF oscillator circuit.

A. Oscillator Design and Analysis

The oscillator is a Colpitts circuit using a VHF silicon JFET (Siliconix type J310). The circuit is shown in Fig. 3. Coupling to other oscillators and injection power sources was made to the gate through the injection node indicated. The oscillator output was taken from an inductive coupling loop feeding the indicated phase monitor output. The load was the high-impedance input of a vector voltmeter which consumed a negligible amount of power.

For purposes of computer simulation, the oscillator was characterized so that it could be modeled by the equivalent circuit of Fig. 1. This process began with the identification of an injection node in the oscillator. This node should be chosen so that a signal of the desired injection power level successfully synchronizes the oscillator over the desired locking bandwidth. In a feedback-loop type of oscillator, the injection node should be a low-level point in the loop to give maximum locking bandwidth. In the case of the Colpitts circuit, we identified the gate terminal as the proper location for the injection node.

Once the injection node was identified, the equivalent circuit values of C and the negative conductance function $G_D(A)$ were determined. The experimental technique used was a modified load-pulling measurement in which a variable complex admittance $Y_{ext} = G_{ext} + jB_{ext}$ was connected to the injection node. As Y_{ext} was varied, the resulting frequency and amplitude data were plotted against B_{ext} and G_{ext}, respectively. The resulting plots of amplitude versus G_{ext} (Fig. 4) and frequency versus B_{ext} (Fig. 5) would be single lines if there were no variation of device reactance B_D with amplitude A. The slight $B_D(A)$ dependence present causes the plots to be narrow closed loops, which were approximated by single-valued functions of a single variable in the computer analysis. For $G_{ext}(A) = -G_D(A)$, a two-piece curve fit shown by the dashed line in Fig. 4 was used.

The plot of frequency versus B_{ext} is used to find the reactance of the equivalent tank circuit. Only the equivalent tank capacitance C is needed for the analysis, since L is automatically chosen to resonate the tank at the

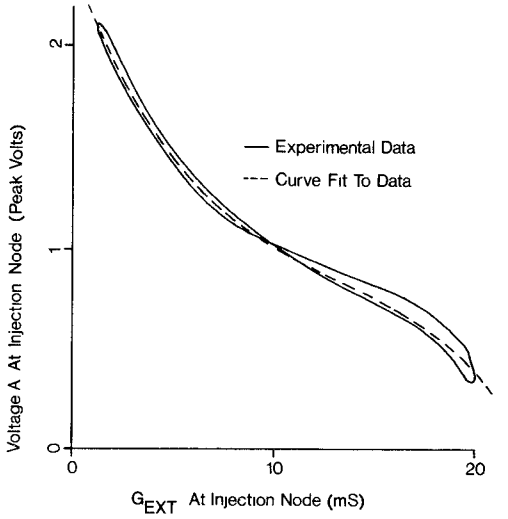

Fig. 4. Amplitude A (peak volts at injection node) versus real part of oscillator load G_{ext}.

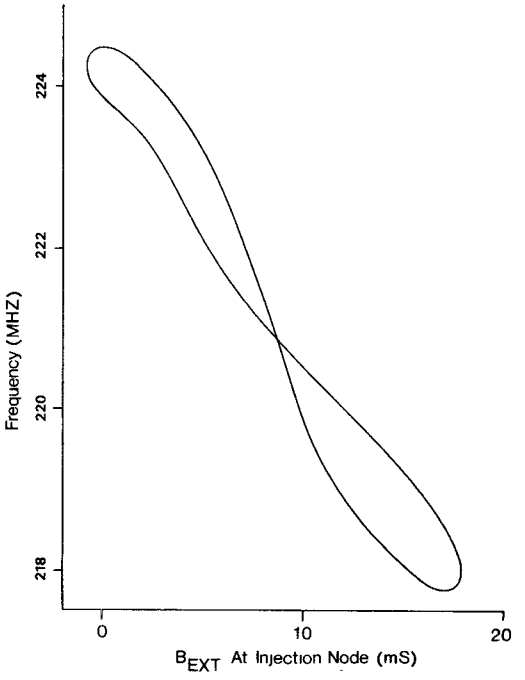

Fig. 5. Frequency f (MHz) versus imaginary part of oscillator load B_{ext}.

free-running frequency f_0. The equivalent capacitance can be found from the average slope $\Delta f/\Delta C_{ext}$ of the curve in Fig. 5

$$C = \frac{-f_0}{2(\Delta f/\Delta C_{ext})}. \tag{9}$$

The value for C thus obtained from the data of Fig. 5 is approximately 212 pF.

The equivalent capacitance measured in this way does not in general have a direct physical counterpart, since its value is an expression of the way the entire circuit responds to external reactive loading on the injection port. The *external* Q of the oscillator is the ratio of equivalent capacitive reactance $\omega_0 C$ to conductance G_{ext}

$$Q_{ext} = \frac{\omega_0 C}{G_{ext}}. \tag{10}$$

For a given value of G_{ext}, a higher Q_{ext} means that the oscillator's frequency is less subject to pulling by means of external susceptance. For a single oscillator, the maximum injection-locking range is a function of Q_{ext}, injection power P_{inj}, and oscillator power P_{osc} delivered to G_{ext} [7]

$$\left|\frac{\Delta\omega}{\omega_0}\right|_{max} = \frac{k}{Q_{ext}}\sqrt{\frac{P_{inj}}{P_{osc}}} \tag{11}$$

where k is a constant of order unity that depends upon the nature of the nonlinear functions $G_D(A)$ and $B_D(A)$. Equation (11) shows that too high an external Q will limit the range over which locking can be achieved. Fortunately, most oscillators using only planar circuit elements have relatively low external $Q(Q_{ext} < 100)$. Although it may be possible to employ high-Q oscillators using such frequency-control devices as YIG's or dielectric resonators, special precautions to insure uniformity of free-running frequencies would be necessary.

B. Inter-Injection-Locked Cascade Design

Once the oscillators were characterized so that their individual injection-locking properties could be modeled adequately, the three-oscillator system design could begin. Our goals for the VHF system were a) to couple the three oscillators so that, with the injection currents in phase $(\theta_1 = \theta_3 = 0)$, all the oscillators are in phase with each other and b) to permit phase steering so that a phase shift of the right-hand injection signal θ_3 with respect to θ_1 causes a linear progression of phase shift from one oscillator to the next.

We began with computer analyses of two free-running oscillators coupled by a real conductance $(B_C = 0)$. Each oscillator was modeled by the equivalent circuit of Fig. 1, in which experimentally determined values for L, C, and $G_D(A)$ were used. The two oscillators were initially assumed to be identical, and the injection current sources were set at zero. A two-oscillator system similar to this was studied by Schlosser [8], but his work emphasized noise behavior, which we have not addressed. In our case, the computer simulation showed that for any realistic set of initial conditions and coupling conductances, the steady state of the two-oscillator system was one in which the oscillator voltages were in phase with each other.

When the injection current sources were introduced and made to be in phase, the two oscillators merely locked to the injection current phase as a single oscillator would. Finally, when the two injection sources were set so that a phase difference existed between them, the phases of the oscillators ϕ_1 and ϕ_2 arranged themselves symmetrically about the average phase $(\theta_1 + \theta_2)/2 = \theta_{AV}$. This behavior is shown in the vector diagrams of Fig. 6, in which the phase difference $\theta_2 - \theta_1$ of the injected currents varies from $-180°$ to $+180°$. For a relatively small coupling

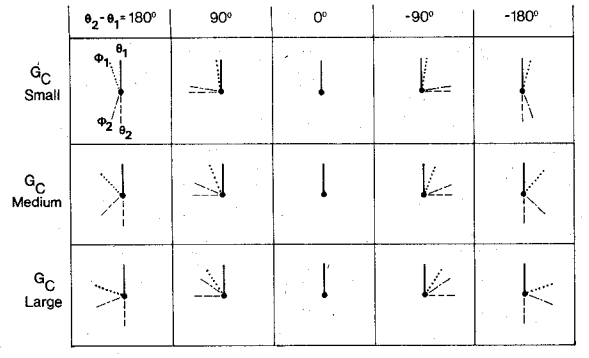

Fig. 6. Phase relationships in the two-oscillator system for $\theta_2 - \theta_1 = 0$, $\pm 90°$, and $\pm 180°$.

conductance, the phase of each oscillator remains near its respective injection source phase, but is pulled slightly towards θ_{AV} by the current flowing through G_c. As the injection phase difference varies, the angular difference $\phi_2 - \phi_1$ between the oscillators remains at all times proportional to the injection phase difference $\theta_2 - \theta_1$. The constant of proportionality is determined by the characteristics of the oscillators and by the ratio of G_c to I/A, where I is the injection current amplitude and A is the oscillator voltage amplitude. If G_c is increased, the tighter coupling is evidenced by the oscillator phases moving closer to each other, as the second and third rows in Fig. 6 illustrate.

When a ladder network of more than two identical oscillators is studied in simulation, the steady-state oscillator phases show an essentially uniform progression from one oscillator to the next. This progression is proportional to the difference in phase between the two injection signals applied to the ends of the network. Since a uniform phase progression from one antenna element to the next is a common requirement of phased antenna arrays, this behavior is extremely interesting. The conventional techniques of generating the required phases require a relatively complex and lossy phase-shifting network for each antenna, which is sometimes difficult to integrate monolithically. It was therefore decided to construct a model system to demonstrate the phase control of three sources by means of a phase change in only one injection power input.

Accordingly, a three-oscillator system was designed around the VHF oscillators described above. Although in the computer simulation we assume that the coupling element is a simple resistor, the need for dc blocking and connectors between oscillators made the actual coupling network somewhat more complex. Fig. 7 shows the experimental system of oscillators together with the injection power source. The coupling network shown in Fig. 7(a) was designed to produce an equivalent series coupling admittance of $Y_c = 2.3$ mS. When the system was driven by an available power of -5 dBm at each end, the computer simulation predicted the phase and amplitude behavior shown in Fig. 8. As the injection phase difference $\theta_3 - \theta_1$ increases, the oscillator phases distribute themselves symmetrically about θ_{AV}, which is the same as ϕ_2 for the three-oscillator case. The associated amplitudes A_1, A_2, and A_3 fall slightly as the phase shift increases, but the maximum change is less than 1 dB, since amplitude has only a second-order dependence on the injection phase difference.

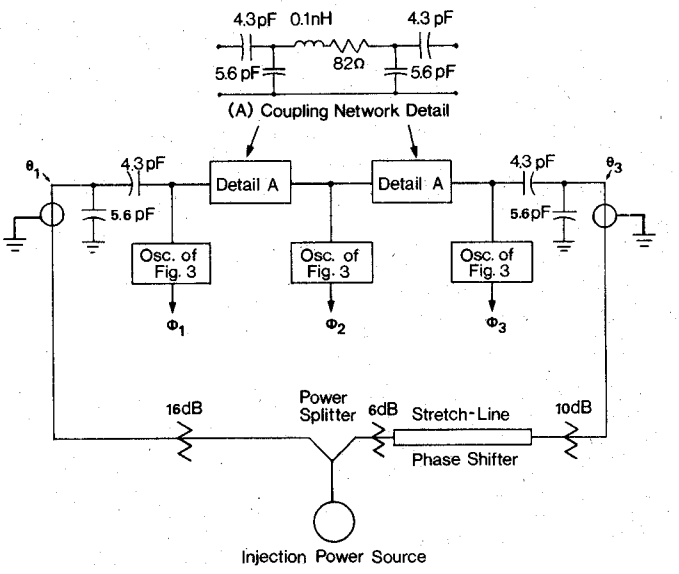

Fig. 7. Experimental oscillators of Fig. 3 coupled via coupling networks (A) and driven by injection signals of phase θ_1 and θ_3.

In the experiment, the injection phase difference was controlled by mechanical adjustment of a coaxial stretch line. The possibility of oscillator–oscillator coupling through means other than the desired paths was reduced by enclosing each oscillator and coupling network in a separate shielded housing. Coupling through the crystal-controlled injection source was prevented by the 20-dB isolation shown by the power splitter on the output of the source, plus 16 dB of attenuation in each leg. The phase of each oscillator was measured by a vector voltmeter whose phase reference was driven by a tap from the injection source, which was unaffected by adjustments in the setup. Slight differences in the phase characteristics of the oscillators' phase monitor outputs were noted and compensated for.

C. Experimental Results

Up to this point, all oscillators have been assumed to be identical. While this condition can never be attained in practice, it can be approached with careful manual adjustments of each oscillator in isolation. When oscillators so tuned are connected together in a system, the reactive loading of the coupling circuits will detune the oscillators slightly from the desired identical condition, since the end oscillators see a slightly different load than the center oscillator. This problem is one cause of possible disagreement between theory and measured results.

Another problem concerned the coupling network. Despite efforts to synthesize a purely real coupling resistance, tests of the coupling networks after completion of the system indicated that the equivalent coupling admittance Y_c was closer to $1.55 - j0.42$ mS, rather than the desired purely real 2.3 mS. The reactive component leads to fur-

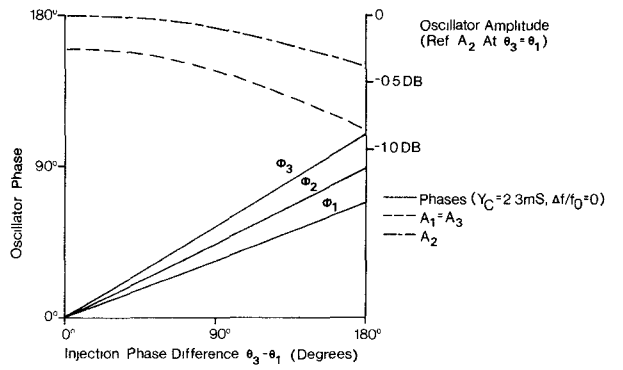

Fig. 8. Predicted phases and amplitudes versus injection phase difference $\theta_3 - \theta_1$ for model of Fig. 7 ($Y_c = 2.3$ mS, $P_{inj} = -5$ dBm).

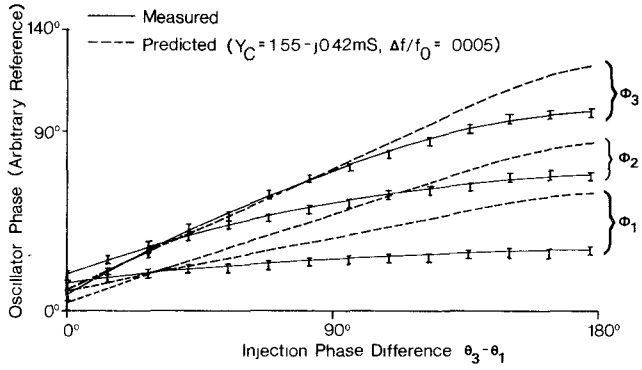

Fig. 9. Predicted phases (dashed lines) and measured phases (solid lines) of oscillators in experimental system of Fig. 7 versus injection phase difference $\theta_3 - \theta_1$ ($Y_c = 1.55 - j0.42$ mS, $P_{inj} = -5$ dBm).

ther detuning and asymmetry in the phase characteristics, as the following data show.

A number of experimental trials were run in which the oscillator tuning was varied quasi-randomly before each trial. A typical set of phase data is shown in Fig. 9 (solid lines). Residual interactions among the oscillators made it difficult to begin the trial with all phases exactly equal, although tuning to within $\pm 5°$ was routinely achieved. As the injection phase difference was increased, the proper phase relationship $\phi_3 > \phi_2 > \phi_1$ was obtained, and the phase progression between oscillators increased in rough proportion to the injection phase difference. Disagreement between the experimental data of Fig. 9 and the initial theoretical prediction of Fig. 8 was obvious, however.

In an attempt to simulate some of the experimental complications, the computer simulation was rerun using the measured value of $Y_c = 1.55 - j0.42$ mS, and detuning all three oscillators from the injection frequency by 0.5 percent. The predictions of this modified simulation are shown in Fig. 9 as dashed lines. Although quantitative agreement is still not obtained, the phase crossovers at low phase differences and the downward concavity of the experimental phase curves at high phase differences are present in the modified simulation. The crossovers are the effects of detuning, and it is suspected that the nonlinear behavior of the phase curves is associated with the reactive component of the coupling admittance Y_c. Considering that the oscillators were not designed to exhibit especially uniform injection-locking characteristics, their performance in a phase-control system of this type is encouraging, although refinements in both the theoretical model and the experimental methods are clearly required.

IV. Extension to Microwave Frequencies

The preceding discussions have shown that inter-injection-locked oscillators function at VHF. We will now show why inter-injection-locking should be a highly viable technique well into the millimeter-wave range and why it is suited to both hybrid and monolithic integrated circuits.

A. Design Considerations

The oscillators in the demonstration system used a lumped-element Colpitts circuit incorporating a JFET. A GaAs MESFET could be substituted in a distributed-element circuit without any fundamental changes. Coupling and biasing techniques would be altered, but the oscillator measurements needed to extract design data would differ only in detail. Proper selection of active elements for the operating frequency is assumed.

At frequencies above 30 GHz, the dominant solid-state high-power sources are two-terminal devices, such as Gunn-effect diodes and IMPATT diodes. Since our analysis is based upon expressions originally developed for broad-band two-terminal negative-resistance devices, millimeter-wave inter-injection-locked system designs should present no unusual analytical difficulties. Although the low impedance levels required by high-power IMPATT's tend to make planar designs difficult, our theory can be adapted to cavity oscillators as well as planar circuits. In fact, the basic inter-injection-locking concept has been demonstrated in the linear array of semiconductor lasers at infrared wavelengths tested by Scifres *et al.* [9], although their work was not cast in terms of oscillator equivalent circuits.

More recently, an experiment at *X*-band was carried out by Dinger *et al.* [10] in which three IMPATT diodes coupled to three microstrip patch antennas were synchronized from only one injection source. Parasitic injection locking of the two outer devices was achieved through inter-antenna coupling. Although differing in some respects from the concepts described in this paper, Dinger's experiment demonstrates the feasibility of using the intrinsic inter-element coupling in a phased array to control oscillator phases.

Our system analysis has assumed that the admittance parameters of the coupling network are constant with frequency. This assumption will be valid unless the system's injection signals are frequency- or phase-modulated over a relatively wide bandwidth. If necessary, frequency-dependent coupling may be incorporated into the model.

B. Frequency Errors and Tuning

The oscillators in the experimental system incorporated tuning capacitors which were adjusted to remove residual

inequalities in the oscillators' free-running frequencies. Although limited amounts of adjustment are possible in hybrid microwave circuits, postmanufacture tuning is undesirable in hybrid circuits and virtually impossible with monolithic microwave integrated circuits (MMIC's). What are the implications of this problem for inter-injection-locked oscillator systems?

We have made a preliminary investigation of this problem by examining the computer-simulated behavior of a number of systems whose oscillators' free-running frequencies are determined by a random number generator. No claim of statistical significance is made for the outcome of these investigations, since the sample sizes are too small and the results are too easily influenced by several variables to be of generaly applicability. Rather, we will show the qualitative effects of random frequency errors using typical values for our cases.

A common situation is that in which the free-running frequencies of a group of oscillators are statistically distributed about a mean frequency $\langle f \rangle$ in a normal (Gaussian) distribution having a standard deviation σf. In an inter-injection-locked system, an oscillator's steady-state phase error for a given frequency error is proportional to Q_{ext}, so the situation is improved by going to lower external Q's. For our statistical study, we used the same VHF oscillator circuit model as above, except that the external Q was lowered from its actual value of about 200 to 50, a value typical of many IMPATT oscillators. We assumed a normalized frequency deviation $\sigma f/\langle f \rangle = 0.001$. This means that, for example, if the mean frequency $\langle f \rangle$ is 10 GHz, 90 percent of the oscillators will have free-running frequencies that fall within ± 16.5 MHz of 10 GHz. Frequency tolerances on this order for planar IMPATT oscillators on a polyimide substrate have been reported by Bayraktaroglu [11]. Ten trials with this normally distributed frequency error using four, eight, and 16 oscillators were examined for their steady-state phase values. The results for the four- and eight-oscillator trials are shown in Fig. 10(a) and (b), respectively. The four-unit trials all converged to steady-state phase errors of less than $\pm 15°$ from the ideal zero-phase-error case. Since the oscillators near the center of the eight-unit system "see" less of the injection signal and more of the random phase errors of the intervening oscillators, one would expect the average phase deviations to be larger, and Fig. 10(b) shows that this is indeed the case. The 16-unit system is not shown because 70 percent of the trials converged to an undesirable mode in which the phase error progresses through one complete cycle from one end of the array to the other. For a given external Q, the effects of frequency errors can be reduced by increasing the coupling conductance G_c and the injection current I in proportion. Since injection power increases as I^2, however, this is an inefficient way to reduce phase errors.

The issue of undesirable modes has been addressed by others, notably Kurokawa [5]. An N-oscillator system can have in general N possible modes of operation, only one

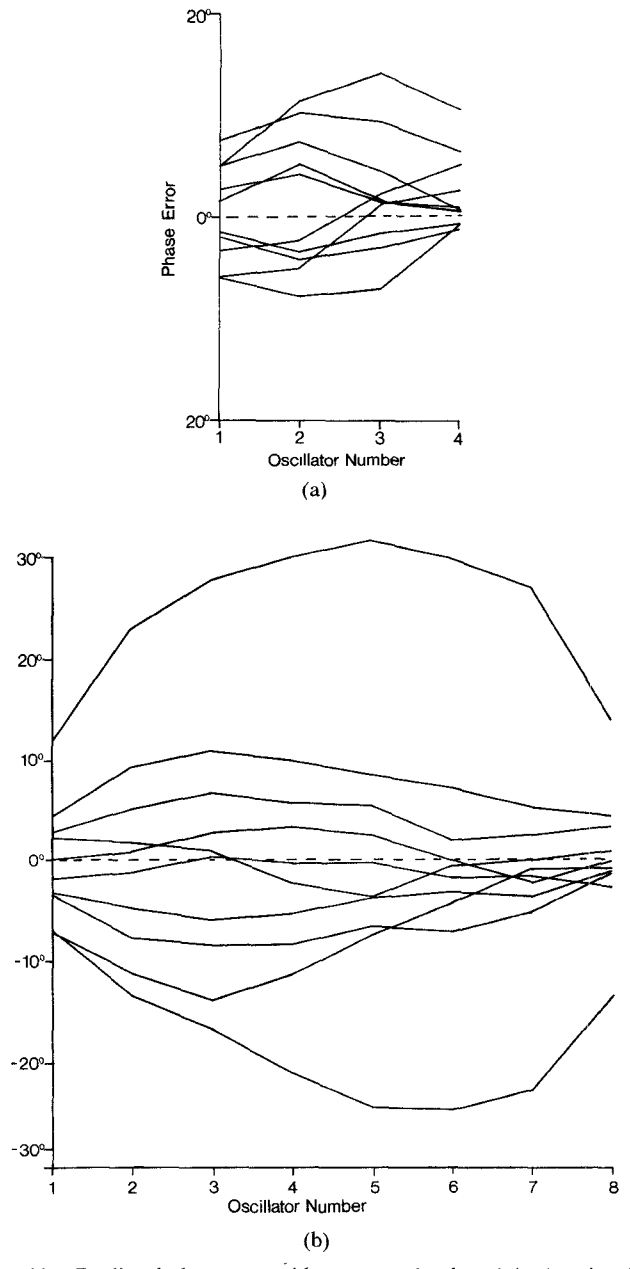

Fig. 10. Predicted phase error with respect to in-phase injection signals, random frequency errors having $\sigma f/\langle f \rangle = 0.001$. (a) Four-oscillator system. (b) Eight-oscillator system.

of which is the desired mode. The purely resistive coupling conductances in our chosen system topology appear to discriminate against modes having a large phase progression per oscillator, since the power dissipated in the coupling network for undesired modes rises, making the desired mode energetically favorable. The reasonably small loss in the coupling networks is the price paid for mode stability. Instability of long cascades could be alleviated by providing appropriately phased injection signals at evenly spaced points within the cascade, as well as at either end. The limiting case of this approach is to provide each oscillator with its own source, but this defeats the purpose of letting the oscillators synthesize the desired phase progression.

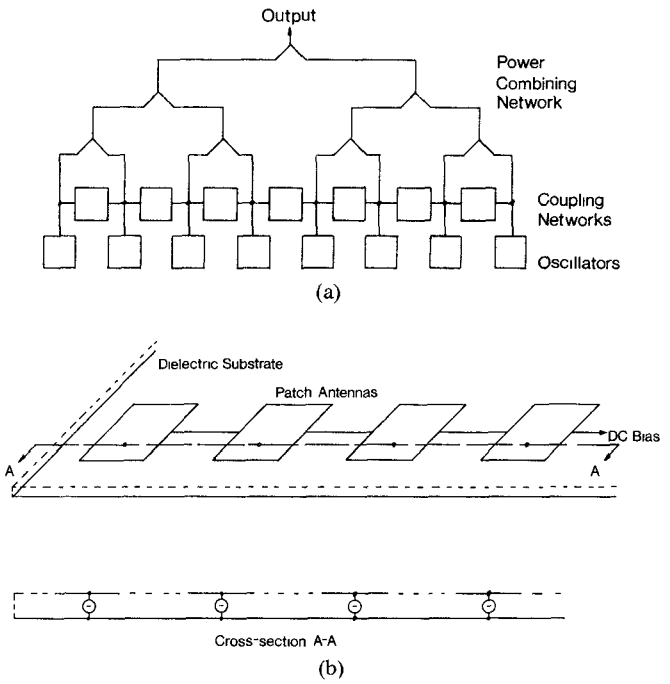

Fig. 11. (a) Inter-injection-locked oscillators driving planar power combiner. (b) Proposed linear phased array driven by inter-injection-locked oscillators.

V. Future Applications of Inter-Injection-Locked Oscillators

A. Power Combining

In Fig. 11(a), we illustrate a proposed configuration of inter-injection-locked oscillators feeding a planar power combiner. As in previous designs, the coupling networks are designed to provide purely real coupling admittances between the injection nodes of adjacent oscillators. If phase coherence with an external reference signal is required, injection power may be introduced into the two end oscillators, thus saving the expense and space required for an N-way power divider, since only two injection inputs are needed.

B. Quasi-Optical Power Combining

Above frequencies at which planar waveguiding media such as microstrip become increasingly lossy, it is possible to eliminate such transmission loss by combining an antenna and oscillator into one unit [12]. In this case, the antenna will act as a) a resonant element, b) a coupling mechanism between oscillators, and c) a transition to the lossless medium of free space, where quasi-optical power combining takes place. Recent advances in the calculation of inter-element coupling in planar phased arrays [13] make it possible to know the coupling characteristics of a given array configuration in advance. The parasitic injection-locking system referred to above [10] has shown that inter-antenna coupling is usable for injection-locking purposes. Fig. 11(b) shows a proposed linear array of oscillator devices feeding a patch antenna array. The dc bias line interconnects the elements at points of minimum electric field. An array of such units running in phase could be focused through space to a receiving horn, thus avoiding losses associated with waveguide or microstrip power-combining circuitry. The advantages of this approach would have to be balanced against losses due to imperfect phase control in a given inter-injection-locked system.

C. Steerable Phased Arrays

A key issue in the application of inter-injection-locked oscillators to steerable-phase transmitting arrays is the maximum phase progression per oscillator obtainable with this technique. As the phase progression per oscillator approaches 90°, the coupling between adjacent oscillators approaches zero, since the coupling currents from the two oscillators on either side of a given unit will cancel out. The phase progression per oscillator Θ_{max} will therefore always be less than 90°, although our experimental unit demonstrated that progressions on the order of 45° are easy to obtain, and computer simulations imply that 60° is possible before an undesirable mode occurs, depending on the external Q of the oscillators. The maximum one-sided beam steering angle Γ_{max} in a linear array is related to the maximum phase progression per element Θ_{max} and the element separation ϕ (in electrical degrees) by

$$\Gamma_{max} = \sin^{-1}\left(\frac{\Theta_{max}}{\phi}\right). \tag{12}$$

Typical element spacings of one-half free-space wavelength ($\phi = 180°$) and $\Theta_{max} = 60°$ give a beam steering Γ_{max} of $\pm 20°$. Larger angles are possible with smaller spacings, which can be obtained with physically small radiators such as patch antennas on high-dielectric constant substrates.

Another issue concerns the rate at which the beam steering angle can be changed without excessive phase error or loss of lock, since there is a time constant associated with the process of injection locking. As an example, we show in Fig. 12 the results of a computer simulation of the phase of the injection signal and of each oscillator in a five-element system as the phase difference between injection signals was slewed from 0° to 270°. In Fig. 12(a), the injection phase change was completed in 1 μs. The oscillator phases were able to keep pace, and the system reached a steady state of phases in the desired equally spaced condition. In Fig. 12(b), the slew rate was increased to complete the change in only 0.5 μs, and the oscillator phases lagged behind and lapsed into an undesired mode. A study of the linearized system using state-variable methods has begun with the aim of obtaining closed-form expressions for the system response to phase modulation of the injection inputs.

The inter-injection-locked concept can be extended to two-dimensional arrays as long as the inter-oscillator coupling can be accurately modeled. In a rectangular two-dimensional array, for example, each unit could be coupled to its four nearest neighbors in a square element pattern, and injection power could be provided at the corners and perhaps the edges of the array. Two-dimensional arrays should also show graceful degradation in the case of isolated oscillator failures.

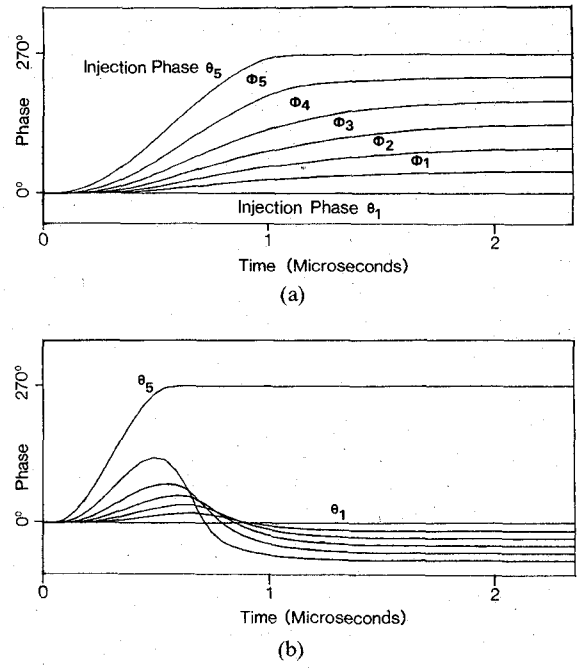

Fig. 12. Computer simulation of five-oscillator-system phase tracking in response to an injection phase slewing of 180° at one end. (a) Phase slew time = 1 μs. (b) Phase slew time = 0.5 μs.

Inter-injection-locked oscillators could also be applied to receiving phased arrays, although the frequency shifting, transmit–receive switching, and phase-matched mixers needed would make this approach less straightforward than a transmitting array.

VI. Conclusions

Presentation of the inter-injection-locking concept has been followed by an experimental demonstration of a working system. Although the concept was demonstrated at VHF, there are no limitations to its applicability at all microwave frequencies and into the millimeter-wave region, since the basic effect has also been demonstrated at optical wavelengths. Applications include, but are not limited to, power combining of solid-state device outputs, quasi-optical power combining, and steerable phased arrays. It is hoped that this study will serve as a stimulus to further investigations of what promises to be a very useful system concept.

Acknowledgment

The author is grateful to Prof. R. W. Jackson for many stimulating discussions, and for the assistance of D. Ringheiser and especially J. F. Hubert, Jr., whose enthusiasm and interest were essential during the early phases of this work.

References

[1] A. H. Al-Ani, A. L. Cullen, and J. R. Forrest, "A phase-locking method for beam steering of active array antennas," *IEEE Trans. Microwave Theory Tech.*, vol. MTT-22, pp. 698–703, June 1974.

[2] R. Adler, "A study of locking phenomena in oscillators," *Proc. IRE*, vol. 34, pp. 351–357, June 1946.

[3] R. C. Mackey, "Injection locking of klystron oscillators," *IRE Trans. Microwave Theory Tech.*, vol. MTT-10, pp. 228–235, July 1962.

[4] K. Kurokawa, "Noise in synchronized oscillators," *IEEE Trans. Microwave Theory Tech.*, vol. MTT-16, pp. 234–240, Apr. 1968.

[5] K. Kurokawa, "The single-cavity multiple-device oscillator," *IEEE Trans. Microwave Theory Tech.*, vol. MTT-19, pp. 793–801, Oct. 1971.

[6] K. Kurokawa, "Some basic characteristics of broadband negative resistance oscillator circuits," *Bell Syst. Tech. J.*, vol. 48, pp. 1937–1955, July–Aug. 1969.

[7] K. Kurokawa, *An Introduction to the Theory of Microwave Circuits*. (New York: Academic Press, 1969), p. 388.

[8] W. O. Schlosser, "Noise in mutually synchronized oscillators," *IEEE Trans. Microwave Theory Tech.*, vol. MTT-16, pp. 732–737, Sept. 1968.

[9] D. R. Scifres, W. Streifer, and R. D. Burnham, "Experimental and analytic studies of coupled multiple stripe diode lasers," *IEEE J. Quantum Electron.*, vol. QE-15, pp. 917–922, Sept. 1979.

[10] R. J. Dinger, D. J. White, and D. Bowling, "A 10 GHz space power combiner with parasitic injection locking," in *IEEE 1986 Int. Microwave Symp. Dig.*, June 2, 1986, Paper G-2 (Baltimore, MD).

[11] B. Bayraktaroglu, "Monolithic IMPATT diodes for millimeter wave applications," presented at the Tenth Int. Conf. on Infrared and Millimeter Waves, Lake Buena Vista, FL, Dec. 1985.

[12] G. Morris, H. J. Thomas, and D. L. Fudge, "Active patch antennas," presented at the 1984 Military Microwave Conf., London, England, Sept. 1984.

[13] D. M. Pozar, "Input impedance and mutual coupling of rectangular microstrip antennas," *IEEE Trans. Antennas Propagat.*, vol. AP-30, pp. 1191–1196, Nov. 1982.

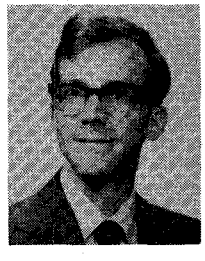

Karl D. Stephan (S'81–M'83) received the B.S. degree in engineering from the California Institute of Technology, Pasadena, CA, in 1976, and the M. eng. degree from Cornell University, Ithaca, NY, in 1977.

In 1977, he joined Motorola, Inc., in Fort Worth, TX. From 1979 to 1981, he was with Scientific-Atlanta, Atlanta, GA, where he engaged in research and development pertaining to cable television systems. After working at Hughes Aircraft in the summer of 1982 as a Student Engineer, he received the Ph.D. degree in electrical engineering from the University of Texas at Austin in 1983. In September 1983, he joined the faculty of the University of Massachusetts at Amherst, where he is presently Assistant Professor of Electrical Engineering. His current research interests include the application of quasi-optical techniques to millimeter-wave circuits and subsystems.